

Catenated and Spirocyclic Polychalcogenides from Potassium Carbonate and Elemental Chalcogens †

Phil Liebing,^a Marcel Kühling,^a Claudia Swanson,^a Martin Feneberg,^b Liane Hilfert,^a Rüdiger Goldhahn,^b Tristram Chivers,^c and Frank T. Edelmann^{*,a}

Received 00th March 2018,
Accepted

DOI: 10.1039/x0xx00000x

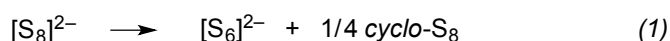
www.rsc.org

The reaction of potassium carbonate with elemental sulfur or selenium in acetone in the presence of [PPN]Cl produces *catena*-[S₁₂]²⁻, the longest structurally characterised polysulfide dianion, or *spiro*-[Se₁₁]²⁻ as ion-separated [PPN]⁺ salts.

Introduction

The critical role played by polysulfide dianions [S_n]²⁻ and related radical monoanions [S_n]^{•-} across the chemical, physical and biological sciences,¹ notably in the development of lithium-sulfur batteries,² in biological signaling involving NO,³ in geochemical processes including metal transport,⁴ and as reagents for the synthesis of organosulfur compounds,^{1,5} has re-generated interest in the fundamental chemistry of these simple homoatomic species. Although small, acyclic radical monoanions [S_n]^{•-} (*n* = 2,3,4) are known to be stabilised in zeolitic matrices,^{1,6} the only single-crystal structural characterisation of these paramagnetic species is the hexasulfide (*n* = 6) in [PPh₄]₂S₆, which has a cyclic structure with two long S–S bonds (263.3 pm) connecting two S₃ units.⁷ However, DFT calculations yield a global minimum structure of C₂ symmetry with only one long S–S bond (294.3 pm).⁸

In the context of sulfur ↔ sulfide redox chemistry the frequently cited eqn. (1)^{2c,d,g} depicts the mass balance, but it does not explain how *cyclo*-S₈ is formed.



As suggested in recent reviews, longer chain polysulfides [S_n]²⁻ (*n* > 8) should be considered for this process.^{1,6} For years, the

longest known dianionic polysulfide chain was the nonasulfide in [K₂(THF)]₂S₉.^{9,10} Very recently, the isolation and structural characterization of the first decasulfide dianion salt, [(222-cryptand)K]₂S₁₀, was reported by Wang and co-workers.¹¹ An X-ray diffraction study confirmed the anticipated chain structure of the [S₁₀]²⁻ dianion. Interestingly, the synthesis of a deep violet solid claimed to be “[PPN]₂S₁₂” (PPN = (Ph₃P)₂N) has been reported by Seel and co-workers, who have also shown that treatment of this polysulfide with NO or [PPN]NO₂ in acetone or DMF generates the biologically significant, red anion [SSNO]⁻.¹² More recently, Pluth and co-workers demonstrated that this acyclic anion is formed by reaction of NO with a solution of the blue radical anion [S₃]^{•-}, which was generated from *cyclo*-S₈ and [NBu₄][SH] in THF.^{3b} The reaction of *cyclo*-S₈ with [PPN]SH in ethanol had previously been shown to give orange-red [PPN]S₇ in high yield.¹³ Significantly, both [PPN]S₇ and “[PPN]₂S₁₂” produce blue [S₃]^{•-} in acetone or acetonitrile solutions as manifested by a strong absorption at 620 nm in the visible spectrum.^{12,13} Furthermore, the radical anion [S₃]^{•-} has been invoked as the reactive species in recent applications of a mixture of sulfur and an alkali-metal carbonate for the synthesis of a variety of organosulfur compounds.^{1,5}

Seel's identification of “[PPN]₂S₁₂” was based solely on elemental (C,H,N,S) analyses. However, the analytical data also fit the monomeric alternative [PPN]S₆. In this context, we describe here the structural characterization of [PPN]₂S₁₂ (**1**), which is readily prepared from the reaction of sulfur with potassium carbonate in acetone in the presence of [PPN]Cl. We have also applied this simple synthetic protocol to the corresponding selenium system in order to provide a direct comparison with the outcome of the sulfur reaction. In earlier work the reaction of potassium carbonate with *red* selenium in acetone at 23 °C in the presence of [PPN]Cl produced red crystals of [PPN][Se₅C(Se)COME] as a minor product (26% yield); the major product of this reaction, a dark green solid, could not be identified in this earlier study.¹⁴ Inspired by the structural characterization of **1**, we have now determined the solid-state structure of this product by X-ray crystallography and shown it to be [PPN]₂Se₁₁ (**2**).

^a Chemisches Institut der Otto-von-Guericke-Universität, 39106 Magdeburg, Germany. E-Mail: frank.edelmann@ovgu.de.

^b Otto-von-Guericke-Universität, Institut für Physik, 39106 Magdeburg, Germany.

^c Department of Chemistry, The University of Calgary, Calgary, Alberta, T2N 1N4, Canada. E-mail: chivers@ucalgary.ca

† Electronic Supplementary Information (ESI) available: Full experimental and characterization details for **1** and **2**. CCDC (1) and (2). For ESI and crystallographic data in CIF or other electronic format see DOI:

Results and discussion

The dodecasulfide salt $[\text{PPN}]_2\text{S}_{12}$ was prepared by a slight modification of the original procedure published by Seel *et al.*¹² Treatment of a suspension of bis(triphenylphosphoranylidene)ammonium (= PPN) chloride and potassium carbonate in acetone with an excess of elemental sulfur led to a blue colouring, followed by formation of a deep orange-red solution. After standing at r.t. for 3 days, well-formed, dark red-violet crystals of $[\text{PPN}]_2\text{S}_{12}$ (**1**) had formed in the suspension. They were freed from unreacted starting materials by thoroughly washing with water and toluene and finally obtained in 12% isolated yield. After washing with CS_2 to remove the last traces of unreacted elemental sulfur the colour of the crystals changed to an intense red-brown (see ESI). A similar reaction of powdered elemental selenium with potassium carbonate in acetone led to a deep green solution, affording dark greenish-black crystals of $[\text{PPN}]_2\text{Se}_{11}$ (**2**) in 8% isolated yield. The outcome of the reaction was independent of the selenium reagent (red, black or grey), but the least reactive grey selenium required a prolonged reaction time at elevated temperature (several hours in refluxing acetone). For both **1** and **2**, the low isolated yields can be attributed to the retention of significant amounts of product in solution and the likely formation of other polychalcogenides.

Compounds **1** and **2** are moderately soluble in acetone and dissolve well in DMSO without decomposition under inert conditions. The dry solids are not very air-sensitive, but their solutions decompose rather quickly under atmospheric conditions. Both products were fully characterised by elemental analyses, IR, Raman, and NMR spectroscopy, thermal analyses (TG-DTA), and single-crystal X-ray diffraction. The elemental analyses are in good agreement with the proposed compositions, and the ^1H and ^{13}C NMR spectra in $\text{DMSO}-d_6$ confirmed the presence of the PPN^+ cation. Separated PPN^+ cations are present in the solid state as well, as the IR spectra of **1** and **2** are very similar to each other and to that of $[\text{PPN}]\text{Cl}$. In the Raman spectrum of **1**, characteristic vibrational bands of the $[\text{S}_{12}]^{2-}$ dianion were found at 383, 429(sh), 437, 508(sh), 516, and 534 cm^{-1} , which are in the same range as the bands previously observed for the related $[\text{PPN}]_2\text{S}_7$.¹³ Meaningful ^{77}Se NMR data for **2** could not be obtained due to insufficient solubility.

Thermal analysis of **1** under an inert atmosphere of nitrogen revealed two decomposition processes between 188 °C and ca. 390 °C. The observed mass loss corresponds to elimination of two sulfur atoms, presumably to produce $[\text{PPN}]_2\text{S}_{10}$, followed by loss of eight sulfur atoms to give $[\text{PPN}]_2\text{S}_2$ (mass loss found: approx. 22%, calcd. for 10 S: 22.0%). The selenium compound **2** is thermally more stable than **1** and melts without decomposition at 156 °C. Simultaneous decomposition of the anion and the cation occurred in the temperature range 369–435 °C (see ESI for full details).

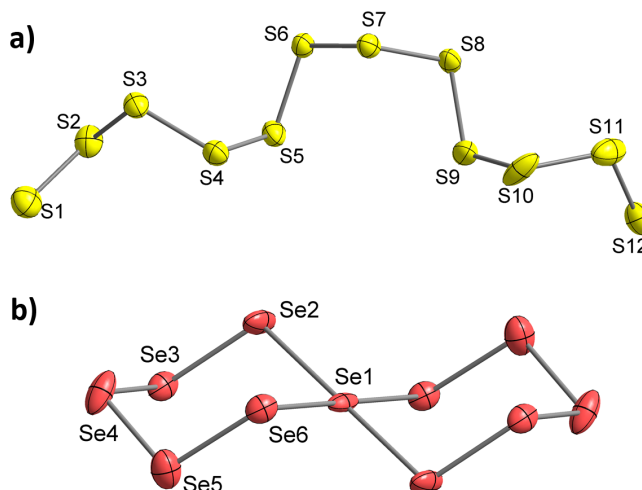


Figure 1. Molecular structures of *catena*- $[\text{S}_{12}]^{2-}$ (a) and *spiro*- $[\text{Se}_{11}]^{2-}$ (b) in the crystals of their respective PPN^+ salts. Displacement ellipsoids drawn at the 50% probability level. Selected bond lengths (pm) and bond angles ($^\circ$) for **1**: S(1)-S(2) 201.3(2), S(2)-S(3) 204.7(2), S(3)-S(4) 207.1(2), S(4)-S(5) 205.5(2), S(5)-S(6) 205.0(2), S(6)-S(7) 204.3(2), S(7)-S(8) 205.3(2), S(8)-S(9) 204.4(2), S(9)-S(10) 207.6(3), S(10)-S(11) 203.4(3), S(11)-S(12) 199.6(3); S(1)-S(2)-S(3) 110.8(1), S(2)-S(3)-S(4) 111.23(9), S(3)-S(4)-S(5) 106.93(9), S(4)-S(5)-S(6) 107.37(8), S(5)-S(6)-S(7) 107.37(8), S(6)-S(7)-S(8) 106.11(8), S(7)-S(8)-S(9) 106.73(8), S(8)-S(9)-S(10) 106.8(1), S(9)-S(10)-S(11) 108.1(1), S(10)-S(11)-S(12) 109.7(1). Selected bond lengths (pm) and bond angles ($^\circ$) for **2**: Se(1)-Se(2) 264.70(4), Se(1)-Se(6) 266.02(4), Se(2)-Se(3) 230.70(7), Se(3)-Se(4) 234.58(7), Se(4)-Se(5) 234.11(7), Se(5)-Se(6) 231.28(7); Se(2)-Se(1)-S(6) 94.12(1), Se(2)-Se(1)-Se(6') 85.88(1), Se2-Se1-Se2' 180, Se2-Se1-Se6 94.12(2), Se2-Se1-Se6' 85.88(2), Se6-Se1-Se6' 180, Se1-Se2-Se3 106.41(2), Se2-Se3-Se4 107.06(2), Se3-Se4-Se5 102.21(2), Se4-Se5-Se6 105.75(3), Se1-Se6-Se5 106.14(2).

Well-formed purple single-crystals of **1** were obtained directly from the original reaction mixture, while greenish-black single-crystals of **2** were grown from a concentrated solution in acetone at r.t. Single-crystal structure determinations of **1** and **2** clearly revealed the presence of separated *catena*- $[\text{S}_{12}]^{2-}$ or *spiro*- $[\text{Se}_{11}]^{2-}$ dianions, respectively (Figure 1). The terminal S-S bonds in **1** are relatively short at 201.3(2) pm (S1-S2) and 199.6(3) pm (S11-S12), while the inner S-S bonds are in the range of 203.4(3)–207.6(3) pm. A CSD search¹⁵ for crystal structures comprising non-coordinated, unbranched $[\text{S}_n]^{2-}$ ions ($n > 6$) revealed four heptasulfides and two octasulfides, in which the terminal S-S bonds are also shorter than the inner S-S bonds (199.5–210.6 pm and 204.0–219.2 pm, respectively). The very recently reported decasulfide dianion $[\text{S}_{10}]^{2-}$ exhibits a similar trend: (terminal S-S 201.5(1) and 202.1(1) pm, inner S-S 202.8(1)–207.6(1) pm).¹¹ The conformation of the $[\text{S}_{12}]^{2-}$ ion in **1** is characterised by the rather regular *syn/anti* sequence *anti-anti-anti-anti-anti-syn-syn-syn-syn-syn* with S-S-S torsion angles in the ranges 70.7(1) to 93.8(1) $^\circ$ (*anti*) and –73.2(1) to –95.1(1) $^\circ$ (*syn*). The situation is therefore similar to that in $[\text{S}_{10}]^{2-}$, which displays an *anti-anti-anti-anti-anti-syn-syn* sequence and comparable ranges of S-S-S torsion angles (72.1(1) to 90.3(1) $^\circ$ and –83.6(1) to –90.8(1) $^\circ$).¹¹ *Cyclo-S*₁₂, the second most stable sulfur

allotrope after *cyclo-S₈*, forms an unstrained twelve-membered ring in the solvate *S₁₂·CS₂* and exhibits only one S-S bond length of 205.4 pm and one torsion angle of 87.2°. There are no significant interactions between the *[S₁₂]²⁻* dianions and the PPN⁺ cations in **1**.

The structural determination of **2** revealed non-interacting PPN⁺ cations and spirocyclic *[Se₁₁]²⁻* dianions. The centrosymmetric *spiro-[Se₁₁]²⁻* dianion in **2** is comprised of two Se₆ rings with typical chair conformations. As found for other salts of *[Se₁₁]²⁻*,¹⁷⁻¹⁹ the central Se atom (Se1, formally Se²⁺) is tetra-coordinated in a slightly distorted square-planar fashion. This Se atom engages in 3c-4e bonding as evidenced by the long Se-Se bond lengths of 264.69(4) pm (Se1-Se2) and 266.02(5) pm (Se1-Se6), which are symmetrical in **2**, as well as in the *[PPh₄]⁺* salt.¹⁹ By contrast, these interactions are strongly asymmetrical in the *[NⁱPr₄]⁺* salt.¹⁷ For the di-coordinate ring-Se atoms, the bonds are much shorter at 230.71(7)–234.58(7) pm, which is comparable to the values observed for *cyclo-S₈*.²⁰

The crystal structure determination of the dodecasulfide salt *[PPN]₂S₁₂* (**1**, PPN = (Ph₃P)₂N) has confirmed the pioneering work by Seel *et al.*, who postulated the formation of *[S₁₂]²⁻* more than 30 years ago.^{12a} The identification of *catena-[S₁₂]²⁻* and the very recent characterisation of *catena-[S₁₀]²⁻*¹¹ add weight to the suggestion that long-chain polysulfides *[S_n]²⁻* (*n* > 8) should be considered as intermediates in the sulfur ↔ sulfide redox process that occurs in lithium-sulfur batteries, *e.g.* the transformation shown in eqn. (1).¹ The current work also indicates that a long chain polysulfide, *e.g.* *[S₁₂]²⁻*, may be the source of *[S₃]^{•-}* in the use of a mixture of sulfur and an alkali-metal carbonate for the synthesis of organosulfur compounds.⁵ Finally, the reaction of elemental selenium with potassium carbonate in acetone is a more convenient route to salts of *spiro-[Se₁₁]²⁻* than previous methods, which involved oxidation of alkali-metal polyselenides (prepared in liquid ammonia) with I₂ in the presence of a large organic cation.¹⁷⁻¹⁹ Significantly, this direct comparison of the outcome of the reactions of potassium carbonate with sulfur or selenium provides a cogent illustration of the predisposition of polyselenides *[Se_n]²⁻* (*n* > 8) to form compact bicyclic structures in preference to the unbranched chains favoured by polysulfides.¹⁰

References

- 1 R. Steudel and T. Chivers, *Chem. Soc. Rev.*, 2019, **48**, 3279–3318 and 2019, **48**, 4338–4338.
- 2 For selected reviews that address the sulfur redox mechanism in Li-S batteries see, (a) K. H. Wujcik, D. R. Wang, A. A. Teran, E. Nasybulin, T. A. Pascal, D. Prendergast and N. P. Balsara, in *Electrochemical Engineering: From Discovery to Product*, eds. R. C. Alkire, P. N. Bartlett and M. Kopev, John Wiley and Sons, 2018, **10**, Ch. 3, pp. 41–74; (b) X. Chen, T. Hou, K. A. Persson and Q. Zhang, *Mater. Today*, 2019, **22**, 142–158; (c) E. Zhao, K. Nie, X. Yu, Y-S. Hu, F. Wang, J. Xiao, H. Li and X. Huang, *Adv. Func. Mater.*, 2018, **28**, 1707543; (d) D. Zheng, G. Wang, D. Liu, J. Si, T. Ding, D. Qu, X. Yang and D. Qu, *Adv. Mater. Technol.*, 2018, **3**, 1700233; (e) G. Zhang, Z-W. Zhang, H-J. Peng, J-Q. Huang and Q. Zhang, *Small Methods*, 2017, **1**, 1700134; (f) R. Xu, J. Lu and K. Amine, *Adv. Energy Mater.*, 2015, **5**, 1500408; (g) M. Wild, L. O'Neill, T. Zhang, R. Purkayastha, G. Minton, M. Marinescu and G. J. Offer, *Energy Environ. Sci.*, 2015, **8**, 3477–3494.
- 3 (a) V. Bogdándi, T. Ida, T. R. Sutton, C. Bianco, T. Ditrói, G. Koster, H. A. Henthorn, M. Minnion, J. P. Toscano, A. van der Vliet, M. D. Pluth, M. Feelisch, J. M. Fukuto, T. Akaike and P. Nagy, *Br. J. Pharm.*, 2019, **176**, 646–670; (b) T. S. Bailey, H. A. Henthorn and M. D. Pluth, *Inorg. Chem.*, 2016, **55**, 12618–12625.
- 4 (a) G. S. Pokrovski, and I. S. Dubrovinsky, *Science*, 2011, **331**, 1052–1054; (b) G. S. Pokrovski, M. A. Kokh, D. Guillaume, A. Y. Borisova, P. Gisquet, J.-L. Hazemann, E. Lahera, W. Del Net, O. Proux, D. Testemale, V. Haigis, R. Jonchiere, A. P. Seitsonen, G. Ferlat, R. Vuilleumier, A. M. Saitta, M.-C. Boiron and J. Dubessy, *Proc. Nat. Acad. Sci.*, 2015, **112**, 13484–13489.
- 5 For recent examples, see (a) M. Wang, Z. Dai and X. Jiang, *Nature Commun.*, 2019, **10**, 2061; (b) H. Huang, Q. Wang, Z. Xu and G.-J. Deng, *Adv. Synth. Catal.*, 2019, **361**, 591–596; (c) H. Huang, Z. Qu, X. Ji and G.-J. Deng, *Org. Chem. Front.*, 2019, **6**, 1146–1150; (d) J-H. Li, Q. Huang, W. Rao, S-Y. Wang and S-J. Ji, *Chem. Commun.*, 2019, **55**, 7808–7811; (e) M. Wang, Q. Fang and X. Jiang, *Org. Lett.*, 2016, **18**, 5756–5759.
- 6 T. Chivers and P. J. W. Elder, *Chem. Soc. Rev.*, 2013, **42**, 5996–6005, and references cited therein.
- 7 B. Neumüller, F. Schmock, R. Kirmse, A. Voigt, A. Diefenbach, F. M. Bickelhaupt and K. Dehnicke, *Angew. Chem. Int. Ed.*, 2000, **39**, 4580–4582.
- 8 R. Steudel and Y. Steudel, *Chem. – Eur. J.*, 2013, **9**, 3162–3176.
- 9 F. Dornhaus, M. Bolte, M. Wagner and H-W. Lerner, *Z. Anorg. Allg. Chem.*, 2007, **633**, 425–428.
- 10 For a review on the structural chemistry of polychalcogenides (S, Se and Te) see, W. S. Sheldrick in *Handbook of Chalcogen Chemistry*, 2nd Edn., Ed. F. A. Devillanova and W.-W. du Mont, RSC Publishing, 2013, Vol. 1, Ch. 9.2, pp. 514–545.
- 11 M. K. Mondal, L. Zhang, Z. Feng, S. Tang, R. Feng, Y. Zhao, G. Tan, H. Ruan, X. Wang, *Angew. Chem. Int. Ed.*, 2019, DOI: 10.1002/anie.201910139.
- 12 (a) F. Seel and M. Wagner, *Z. Naturforsch.*, 1985, **40B**, 762–764; (b) F. Seel, R. Kuhn, G. Simon, M. Wagner, B. Krebs and M. Dratmann, *Z. Naturforsch.*, 1985, **40B**, 1607–1617.
- 13 T. Chivers, F. Edelmann, J. F. Richardson and K. J. Schmidt, *Can. J. Chem.*, 1986, **64**, 1509–1513.
- 14 T. Chivers, M. Parvez, M. Peach and R. Vollmerhaus, *J. Chem. Soc., Chem. Comm.*, 1992, 1539–1540.
- 15 C. R. Groom and F. H. Allen, *Angew. Chem. Int. Ed.*, 2014, **53**, 662–671.
- 16 J. Steidel, R. Steudel and A. Kutoglu, *Z. Anorg. Allg. Chem.*, 1981, **476**, 171–178.
- 17 J. Dietz, U. Müller, V. Müller and K. Dehnicke, *Z. Naturforsch., B*, 1991, **46b**, 1293–1299.
- 18 S.-P. Huang, S. Dhingra and M. G. Kanatzidis, *Polyhedron*, 1992, **11**, 1869–1875.
- 19 (a) M. G. Kanatzidis and S.-P. Huang, *Inorg. Chem.*, 1989, **28**, 5667–4669; (b) B. Krebs, E. Lühns, R. Willmer and F.-P. Ahlers, *Z. Anorg. Allg. Chem.*, 1991, **592**, 17–34.
- 20 O. Voss and V. Janickis, *J. Chem. Soc. Chem. Commun.*, 1977, 834–835.